Broadband dielectric characterization of aqueous saline solutions by an interferometer-based microwave microscope

S. Gu, Tianjun Lin, T. Lasri

Applied Physics Letters

Broadband dielectric characterization of aqueous saline solutions by an interferometer-based microwave microscope

Cite as: Appl. Phys. Lett. **108**, 242903 (2016); https://doi.org/10.1063/1.4953629
Submitted: 24 February 2016 • Accepted: 25 May 2016 • Published Online: 13 June 2016

Sijia Gu, Tianjun Lin and Tuami Lasri

Broadband dielectric characterization of aqueous saline solutions by an interferometer-based microwave microscope

Sijia Gu, Tianjun Lin, and Tuami Lasri[a)]
Institut d'Electronique, de Microélectronique et de Nanotechnologie, CNRS UMR 8520/University of Lille 1, Avenue Poincaré, CS 60069, 59652 Villeneuve d'Ascq, France

(Received 24 February 2016; accepted 25 May 2016; published online 13 June 2016)

The complex dielectric permittivity of aqueous saline solutions has been determined in the frequency range [2–18 GHz] with a home-made near-field microwave microscope. The instrument is built on a vector network analyzer, a matching network, and an evanescent microwave probe. The interferometer-based matching network enables highly reproducible, sensitive, and accurate measurements on the entire frequency band of operation. NaCl solutions concentrations ranging from 0 to 160 mg/ml are investigated at 25 °C. A maximum measurement sensitivity for NaCl concentrations is found to be equal to 2.3 dB/(mg/ml) and 7.7°/(mg/ml) for magnitude and phase-shift, respectively. To translate the measurement data (S parameters) to the corresponding complex permittivities, an inversion procedure based on a simple calibration model is applied. The resulting complex permittivities are found to be in a very good agreement with those calculated by Cole-Cole model. *Published by AIP Publishing*. [http://dx.doi.org/10.1063/1.4953629]

In the last decade, the understanding of the dielectric properties of biological samples such as cells, tissues, and organs has attracted increasing attention owing to their large impact in many physiological, biological, and physical processes.[1,2] The evaluation, especially the local investigation, of the dielectric spectra in the microwave frequency band is expected, for example, to help to visualize the composing elements of biological materials in life sciences.[3] To this end, a well-designed microwave platform that provides high performance in terms of resolution and sensitivity is needed. Conventional microwave resonator methods[4,5] including microstrip structures, cavity resonators, and waveguides have been widely applied to dielectric characterizations. But in this case the frequency band of operation is very limited. Another weakness is that the measurement sensitivity falls rapidly in the presence of high-loss materials such as fluids. However, it is worth noting that methods based on parallel plate capacitors or open-ended coaxial transmission lines have been applied to measure fluids over a broad frequency range.[6] Nevertheless, these approaches involve samples whose size is in the order of tens of square millimeters in terms of surface.[6,7] Recently, microwave microscopy has effectively established its potentials for local dielectric characterization of bio-samples by using sharpened tips.[3,8–11] Nonetheless, most of the microscopes are based on resonators operating in a limited frequency band. Even though some researches have demonstrated dielectric characterizations in a wide frequency range,[12] the sensitivity reported is not equally high in the entire frequency band investigated. Therefore, there is a demand for the development of a bio-sample dielectric spectroscopy.

To this end, we have proposed an interferometer-based microwave microscope offering both spatial resolution at the micro-scale and high measurement sensitivity.[13,14] In this work, we take advantage of the high sensitivity feature of this platform to demonstrate its capability in characterizing bio-samples in a wide and quasi-continuous frequency band [2–18 GHz]. In this purpose, the sample under test selected is a set of saline aqueous solutions. This choice is motivated by the fact that it is quite easy to obtain samples with calibrated concentrations and also because saline aqueous solutions are very commonly used to simulate biological fluids.[15,16] The samples are investigated by using a tapered conductor extruded out of a coaxial connector. Thus, only a quite small volume related to the size of the probe apex is analyzed. In this preliminary study, we are mainly interested in the ability of our platform to perceive a very small variation in the sample under test. This is a first step towards the final objective of quantitative microwave microscopy of biological structures. In the below paragraph, a brief description of the microscope setup is first given. Second, the electromagnetic field distribution induced by the interaction between the probe and the liquid is analyzed. Then, Cole-Cole model is exploited to estimate the complex permittivity of different aqueous saline solutions. Finally, an inversion procedure to retrieve the dielectric properties from the measured data is proposed. As in final point, after a fine study of the measurement sensitivity of the microscope system, the inversion procedure is applied to characterize a set of samples of different saline concentrations [0–160 mg/ml]. The resulting complex permittivities are compared to theoretical values calculated by Cole-Cole model.

Generally, a near-field microwave microscope (NFMM) combines a microwave source (i.e., a vector network analyzer-VNA), an evanescent microwave probe (EMP), and an impedance matching network. In fact, because of the large mismatch between the impedances of the VNA (50 Ω) and the EMP (in the order of kΩ), a matching circuit is required in-between them.[13,14] The circuit proposed is based on an interferometric technique to achieve high measurement sensitivity. The interferometer includes a coupler whose role is

[a)]Author to whom correspondence should be addressed. Electronic mail: tuami.lasri@iemn.univ-lille1.fr

to combine the signals reflected, respectively, by the EMP (Γ_{EMP}) and by the impedance tuner (Γ_{TUN}) involving a variable attenuator and a phase-shifter. Γ_{TUN} is carefully adjusted to compensate Γ_{EMP} by adequately choosing attenuator and phase-shifter positions that lead to a signal with an equal magnitude and an opposite phase-shift when comparing to Γ_{EMP}. The resulting combined signal, close to zero, is the reference signal level. Thus, an extremely small variation of Γ_{EMP} can be detected, leading to a high measurement sensitivity and accuracy. By this process, a very good matching between the EMP and the VNA is achieved. In the technique proposed, the signal variation is measured in transmission mode (S_{21}) to benefit from a high signal-to-noise ratio of the VNA.[17] The device/material to be measured is mounted on an x-y-z stage. In this study, we have only made use of the z-axis of the stage. More information on the instrumentation can be found in Refs. 13 and 14. In particular, the influence of the setting parameters of the platform (S_{21} level, intermediate frequency bandwidth-IFBW, acquisition time and scanning step) on the measurement errors has been carefully studied.[13]

Simulations of the probe-liquid interaction have been performed using ANSYS/HFSS™ software to visualize the electromagnetic field distributions between the probe tip and the liquid under test. For the simulation, an excitation port (50 Ω) is directly connected to the metallic conical probe which is terminated by a semi-sphere (diameter: 260 μm). The simulation data entries for the liquid (ε' and $\tan\delta$) are determined from the Cole-Cole equation. In Fig. 1, the E-field distributions at the cross section along the probe are given for two positions: probe at 300 μm over liquid surface (Fig. 1(a)) and probe immersed into liquid at a depth of 300 μm (Fig. 1(b)). For these tests, the liquid sample is deionized water (DI water: 0 mg/ml) and the frequency is set to 2 GHz.

As displayed in Fig. 1(a), because of the large dielectric constant difference between air ($\varepsilon' = 1$) and water ($\varepsilon' = 77.7$ at 2 GHz), the E-field penetration in liquid is extremely low even at a stand-off distance roughly equal to the apex size of the probe. The main part of the electromagnetic energy is reflected back at the air-liquid interface. The E-field distributions cartography also demonstrates that as water presents higher dielectric losses than free space, the E-field maximum value decreases and the electromagnetic energy dissipation increases in liquid. It is also exhibited that the E-field is strongly spatially confined at the probe end and decays rapidly. This confinement allows very local characterizations. Additionally, when the probe is immersed into water, the impedance mismatch between the probe-liquid system and the excitation port is reduced resulting in a lower reflection coefficient. Another advantage in case of an immersed probe is the immunity to water evaporation process at the liquid surface layer which can largely influence the air-liquid interface and the concentrations of saline solutions.

It is well known that the complex permittivity of materials (ε^*) expresses their abilities to polarize in response to an applied field. The Cole-Cole model (Eq. (1)) has been found to be very efficient for the representation of many systems over a wide frequency band[15,16]

$$\varepsilon^* = \varepsilon' - j\varepsilon'' = \varepsilon_\infty \frac{\varepsilon_s - \varepsilon_\infty}{1 + (j\omega\tau)^{1-\alpha}} + \frac{\sigma_i}{j\omega\varepsilon_0}, \tag{1}$$

ε' and ε'' are, respectively, the real and imaginary parts of the permittivity, ε_∞ and ε_s are the limit of the permittivity at high and low frequencies, σ_i is the ionic conductivity, τ is the relaxation time, α is a distribution parameter, and ε_0 is the permittivity of free space. After the calculation of all these parameters (ε_s, ε_∞, σ_i, τ, and α) at 25 °C, the complex permittivity can be determined. The results for saline concentrations ranging from 0 to 160 mg/ml (0 to 2.74 mol/l) at 2 GHz are presented in Fig. 2.

In Fig. 2(a), the very well-known behavior of the water permittivity is retrieved as a function of frequency. To visualize the frequency-dependent permittivity as a function of saline concentrations, Cole-Cole plots are drawn for 4 concentrations of sodium chloride (Fig. 2(b)). In this figure, ε_∞ (5.8) represents the dielectric constant of infinite frequency (f_∞) and ε_s (77.7) is the static dielectric constant of low frequency (f_s). After this theoretical study of aqueous saline solutions permittivity, a calibration method is proposed to relate the measured transmission coefficient (S_{21}) to the complex permittivity.

As the evanescent waves dominate the near-field of the probe end, a lumped element model can be used to describe the tip sample impedance Z_L. The relation between Z_L and the material permittivity ε^* can be given by[18]

$$Z_L = \frac{1}{i\omega\varepsilon_0\varepsilon^* D}, \tag{2}$$

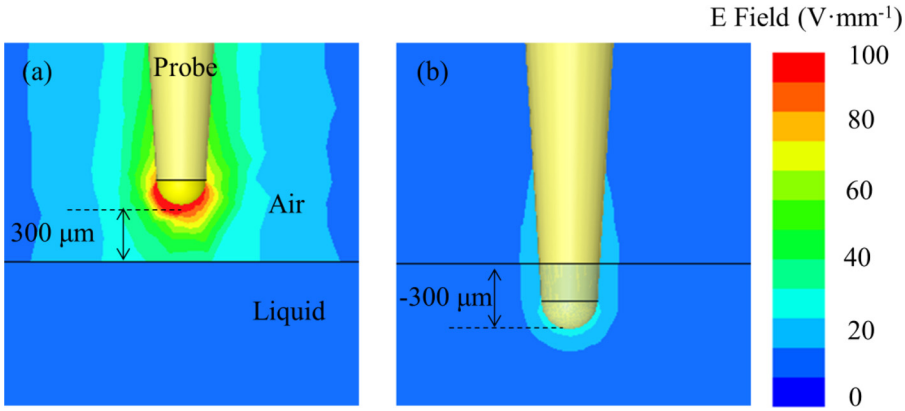

FIG. 1. Numerical simulation (ANSYS/HFSS) of the EMP (apex = 260 μm) electric field magnitude at two probe positions: (a) probe at 300 μm over liquid surface and (b) probe into the liquid at a depth of 300 μm. The images are taken at the cross section along the probe. Liquid under test is DI water. T = 25 °C, F = 2 GHz.

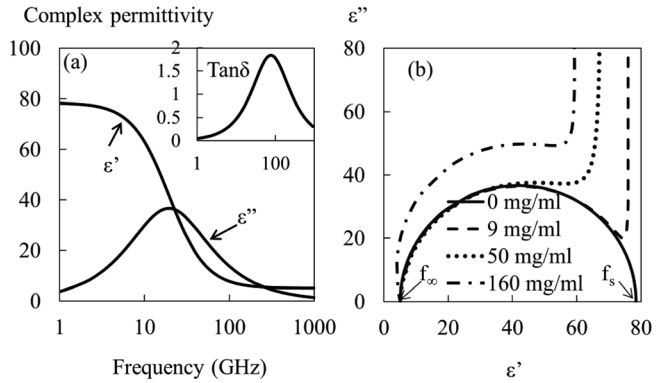

FIG. 2. Complex permittivity of saline solutions based on Cole-Cole model at 25 °C: (a) frequency dependence of the complex permittivity for DI water; tan δ is given in the inset and (b) Cole-Cole plot for different saline concentrations (0, 9, 50, and 160 mg/ml).

where ω is the angular frequency and D is the probe apex size. The reflection coefficient of the probe Γ_{EMP} can be written as a function of Z_L

$$\Gamma_{EMP} = \frac{Z_L - Z_0}{Z_L + Z_0}, \tag{3}$$

with Z_0 the VNA characteristic impedance (50 Ω). Considering the matching network as a whole, an inversion procedure based on the one port calibration protocol can be performed to translate the measured data (S_{21}) to the saline solutions dielectric properties. The complex transmission coefficient S_{21} can be expressed through the probe reflection coefficient Γ_{EMP} in the following form:[3]

$$S_{21} = e_{00} + \frac{(e_{10}e_{01})\Gamma_{EMP}}{1 - e_{11}\Gamma_{EMP}}, \tag{4}$$

e_{00}, e_{11}, and $e_{10}e_{01}$ are three complex error parameters which have to be obtained from the calibration process. These terms can be extracted by measuring three transmission coefficients for three known calibration standards Z_{L1}, Z_{L2}, and Z_{L3} with reflection coefficients Γ_{EMP1}, Γ_{EMP2}, and Γ_{EMP3}. Once these calibration terms are determined, the complex permittivity can be calculated by exploiting Eqs. (1)–(4). One point that makes calibration more difficult is that these error terms change each time the operating frequency is modified. In this study, the inversion procedure is performed by stepping the frequency over the band [2–18 GHz] with a step of 1 GHz.

Previous studies have been dedicated to the evaluation of the errors associated to the platform.[13] It has been found that the errors brought by the instrument can be split into two parts whose sources are electrical and mechanical. In the present case, the mechanical error is not considered because the platform is used in a static mode (probe at a fixed position, no scanning). A standard deviation of the complex transmission coefficient lower than 1.5% (0.5% at 2 GHz (Ref. 13)) has been found over the whole frequency band [2–18 GHz]. For comparable frequency band, this performance is much better than the resonator-based structures.[12]

One of the great advantages of the technique proposed is the different modes offered: non-contact, contact, and

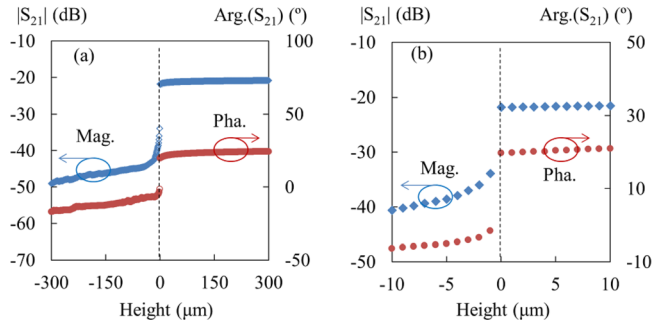

FIG. 3. Transmission coefficient magnitude and phase-shift as a function of probe tip position: (a) from −300 to 300 μm and (b) zoomed region from −10 to 10 μm. Liquid under test is DI water. T = 25 °C, F = 2 GHz, IFBW = 100 Hz, and P_0 = 0 dBm.

immersion. In this study, to guarantee a strong tip-sample interaction, the probe is plunged into the liquid. Nevertheless, one issue related to operation in liquid is the determination of the probe position. The method used to achieve an accurate positioning is as follows. First the probe is immersed in the liquid and the $|S_{21}|$ level is tuned down to the order of −55 dB at 2 GHz by adjusting the impedance tuner. The IFBW is set to 100 Hz and the VNA power level (P_0) is fixed at 0 dBm. To determine the contact position between the tip and the liquid, the probe is placed above the liquid and then pushed towards the liquid surface with a step of 1 μm (minimum displacement allowed by the x-y-z stage with a precision of 0.1 μm) until the tip is immersed in the liquid at a depth of a few hundred microns.

Fig. 3 shows the evolution of the S_{21} with the probe tip position. Thanks to the strong interface effect shown in the simulation study, an abrupt change in both the magnitude and phase-shift of S_{21} can be observed. As illustrated in Fig. 3(a), this frank break defines the 0, the plan that separates two probe statuses: probe in liquid and probe in air. To better locate this position, we zoom the region from −10 μm to 10 μm in Fig. 3(b). A big jump for both magnitude ($\Delta|S_{21}| = 12$ dB) and phase-shift ($\Delta\varphi = 22.1°$) of S_{21} is caused by the passage from liquid to air.

The EMP position is thus very well controlled thanks to the high precision provided by the x-y-z stage. It is also observed in Fig. 3 that when the tip is in air, constant values are measured. This is due to the fact that matching is done in the liquid to obtain a high sensitivity in the immersion mode.

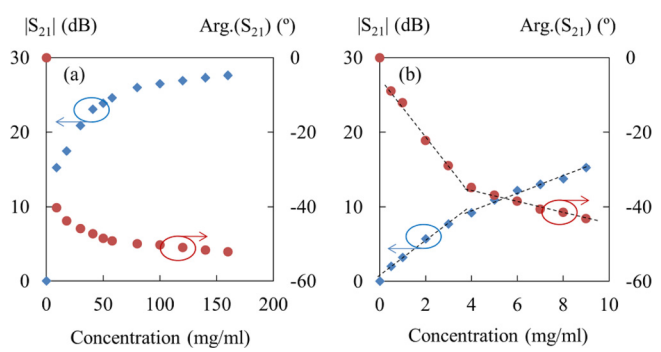

FIG. 4. Measured transmission coefficient for different saline concentrations: (a) 0–160 mg/ml and (b) 0–9 mg/ml. $|S_{21}|$ is tuned to −55 dB considering 0 mg/ml (DI water) as a reference value. F = 2 GHz, T = 25 °C, IFBW = 100 Hz, and P_0 = 0 dBm.

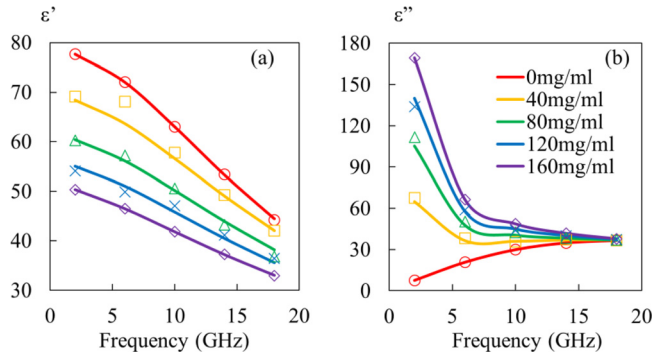

FIG. 5. Frequency-dependent dielectric constant (a) and dielectric losses (b) for different saline concentrations from 0 to 160 mg/ml. Solid lines = values based on the Cole-Cole model. Symbols = values after inversion procedure. T = 25 °C, IFBW = 100 Hz, and $P_0 = 0$ dBm.

The quantitative measurement of sensitivity is given in this part. The probe tip is immersed into the liquid at 300 μm depth. The $|S_{21}|$ level is tuned to −55 dB at 2 GHz considering 0 mg/ml (DI water) as a reference value. The saline solutions concentration influence on the magnitude and phase-shift of S_{21} is highlighted in Fig. 4. Practically, for concentrations from 0 to 160 mg/ml, variations of 27.6 dB and 45.6° for magnitude and phase-shift at 2 GHz are, respectively, observed in Fig. 4(a). Furthermore, thanks to this high sensitivity provided by the interferometric technique, a small variation of concentration from 0 to 9 mg/ml can also be very accurately measured as shown in Fig. 4(b). In the latter, one can distinguish two different linear zones for both the magnitude and phase-shift of S_{21} leading to different sensitivities.

In the concentration range [0–3 mg/ml], the sensitivity is equal to 2.34 dB/(mg/ml) and 7.7°/(mg/ml) for magnitude and phase-shift, respectively. Whereas in the range [3–9 mg/ml], the sensitivity is 1.21 dB/(mg/ml), and 2.13°/(mg/ml), respectively. These sensitivities are much better than those obtained by the typical resonator-based sensor.[4] Indeed, one of the advantages of the method is that the reference level can be adjusted at a desired concentration to enhance the sensitivity around this value. Finally, this procedure has been applied on the whole frequency range [2–18 GHz] with a step of 1 GHz to determine the complex permittivity of a set of saline solutions.

Different saline concentrations [0–160 mg/ml] are characterized in the frequency range [2–18 GHz]. In Fig. 5, the complex permittivities calculated from the measured S_{21} by using the calibration model are compared to the theoretical values based on the Cole-Cole model. Five concentrations [0, 40, 80, 120, and 160 mg/ml] are selected.

First, a good agreement is observed between the dielectric spectra calculated by Cole-Cole model and the values retrieved from the inversion procedure. As shown in Fig. 5(a), the dielectric constant decreases as frequency increases. However, less variation of dielectric constant over the whole frequency band is obtained for higher NaCl concentrations. At lower frequencies (i.e., $F < 5$ GHz), Fig. 5(b) exhibits a big difference between dielectric losses as a function of concentration. The curves gradually evolve towards a constant value (37) at 18 GHz. Actually, this convergence point represents a complete failure for dipole to follow the oscillation of applied electric field beyond which the liquid dipole remains freeze with no effective contribution to the dielectric loss.[15]

This study gives a fine description of the dielectric properties of saline solutions as a function of both NaCl concentration [0–160 mg/ml] and frequency [2–18 GHz] based on a home-made near-field microwave microscope. Thanks to this approach, the measurement sensitivity achieved is higher than the one given by the resonator-based platforms. A maximum measurement sensitivity equal to 2.3 dB/(mg/ml) and 7.7°/(mg/ml) for magnitude and phase-shift, respectively, is found in the range [0–3 mg/ml]. The inversion procedure proposed effectively translates the measurement data (S_{21}) to the dielectric properties (ε' and ε''). This study is a contribution towards quantitative microwave microscopy of biological structures.

[1]M. Habibi, D. P. Klemer, and V. Raicu, Rev. Sci. Instrum. **81**, 075108 (2010).
[2]K. Shiraga, T. Suzuki, N. Kondo, T. Tajima, M. Nakamura, H. Togo, A. Hirata, K. Ajito, and Y. Ogawa, J. Chem. Phys. **142**, 234504 (2015).
[3]S. S. Tuca, G. Badino, G. Gramse, E. Brinciotti, M. Kasper, Y. J. Oh, Z. Rong, R. Christian, H. Peter, and F. Kienberger, Nanotechnology **27**, 135702 (2016).
[4]A. Chahadih, P. Y. Cresson, Z. Hamouda, S. Gu, C. Mismer, and T. Lasri, Sens. Actuators, A **229**, 128 (2015).
[5]J. M. Le Floch, C. Bradac, N. Nand, S. Castelletto, M. E. Tobar, and T. Volz, Appl. Phys. Lett. **105**, 133101 (2014).
[6]M. Stoneman, A. Chaturvedi, D. B. Jansma, M. Kosempa, C. Zeng, and V. Raicu, Bioelectrochemistry **70**, 542 (2007).
[7]C. Gao, B. Hu, P. Zhang, M. Huang, and W. Liu, Appl. Phys. Lett. **84**, 4647 (2004).
[8]M. Farina, A. Di Donato, D. Mencarelli, G. Venanzoni, and A. Morini, IEEE Microwave Wireless Compon. Lett. **22**, 595 (2012).
[9]M. Farina, A. Di Donato, T. Monti, T. Pietrangelo, T. Ros, A. Turco, G. Venanzoni, and A. Morini, Appl. Phys. Lett. **101**, 203101 (2012).
[10]M. C. Biagi, R. Fabregas, G. Gramse, M. Van Der Hofstadt, A. Juárez, F. Kienberger, L. Fumagalli, and G. Gomila, ACS Nano **10**, 280 (2016).
[11]A. Tselev, J. Velmurugan, A. V. Ievlev, S. V. Kalinin, and A. Kolmakov, ACS Nano **10**, 3562 (2016).
[12]T. Alexander, S. M. Anlage, Z. Ma, and J. Melngailis, Rev. Sci. Instrum. **78**, 044701 (2007).
[13]S. Gu, K. Haddadi, A. El Fellahi, and T. Lasri, IEEE Trans. Instrum. Meas. **65**, 890 (2016).
[14]K. Haddadi, S. Gu, and T. Lasri, Sens. Actuators, A **230**, 170 (2015).
[15]Z. Ahmad, *Dielectric Materials* (InTechOpen, 2012), Chap. 1.
[16]A. Peyman, C. Gabriel, and E. H. Grant, Bioelectromagnetics **28**, 264 (2007).
[17]A. O. Oladipo, A. Lucibello, M. Kasper, S. Lavdas, G. M. Sardi, E. Proietti, F. Kienberger, R. Marcelli, and N. C. Panoiu, Appl. Phys. Lett. **105**, 133112 (2014).
[18]S. Anlage, V. Talanov, and A. Schwartz, *Scanning Probe Microscopy: Electrical and Electromechanical Phenomena at the Nanoscale* (Springer, 2007), Vol. 1, p. 215.